Motion energy harvesting and storage system including printed piezoelectric film and supercapacitor

C. Rokaya, P. Schaeffner*, S. Tuukkanen, J. Keskinen and D. Lupo
Tampere University, Korkeakoulunkatu 7, Tampere, Finland 33720
**Joanneum Research Forschungsgesellschaft mbH, Franz-Pichler-Strasse 30, 8160 Weiz, Austria*
*Contact: Chakra.Rokaya@tuni.fi., phone +358-504478515

Abstract—
We report the study of piezoelectric transducer based on the copolymer P(VDF:TrFE) for energy harvesting based on deformation of the film. The bending characteristics, sensitivity, charge generation and frequency response at typical machine component frequencies of printed piezoelectric transducer was studied. Interestingly piezoelectric transducer shows response towards a different level of frequency and the bending forces. As expected, increased frequency and deformation yield increased energy harvesting. A harvester system integrated on flexible foil and comprising a printed piezoelectric element, integrated rectifier and printed supercapacitor was demonstrated, which harvests sufficient energy for low power measurements or radio transmission.

I. INTRODUCTION

Energy harvesting is a method for obtaining or capturing the possible amounts of energy from our surroundings available in the form of heat, motion, mechanic, solar, pressure gradients etc. A large amount of energy in a macro scale can be obtained from solar, wind, kinetic for domestic as well as industrial purposes. Energy harvesting is also a useful and important means of making low power distributed transducers energetically autonomous and environmentally sustainable. [1] Harb mentioned there are a number of approaches to energy harvesting. One way is energy conversion of mechanical to electrical energy using piezoelectric transducer materials. Such harvested energy can be used for low powered systems such as wireless transducers, biomedical implants, military monitoring services, structure-embedded instrumentation, remote weather station, calculators, watches, Bluetooth headsets etc. [2]

A recent trend in electronics has been a decrease of the size and power consumption of devices and components. This has enabled the creation of new applications with low power requirements. Furthermore, environmental issues and imposed regulations are associated with portable energy sources. The use of conventional batteries is not an optimal solution because of the limited cycle life and the requirement for recycling due to problematic materials. Due to advances in low power electronics, harvesting ambient energy and storage in supercapcitors is becoming a viable and more sustainable alternative approach, including piezoelectric harvesting. [3]

Future mobile electronics technologies will focus on light weight, flexible, bendable and stretchable devices as well as large area interactive and learning environments. For such products, flexible piezoelectric materials can play important role both for sensing and energy harvesting. [4] Polyvinylidene fluoride (PVDF) is the most frequently used piezoelectric polymer. It has four phases out of which only the β-phase exhibits spontaneous polarization. It is semi-crystalline (about 50-60% crystallinity) with a repeating unit of (CH2-CF2). The size of the crystallites and chain packing is influenced by annealing. [5] Its piezoelectric properties arise from the strong molecular dipoles within the polymer chain with piezoelectric coefficients (d) in the range of 10-40pC/N. [6] Introducing ca. 20-50% of trifluoroethylene (TrFE), in which one hydrogen is replaced by the slightly larger fluorine, forms a stable copolymer. [7] Energy harvesting from PVDF and its copolymer P(VDF:TrFE) has been reported previously. Bhavanasi *et al.* used bilayer films of P(VDF:TrFE) that generate 4.41μWcm^{-2}. [8] Dey *et al.* showed that electrical response of PVDF:TrFE nanofibers increased with excitation frequency. [9] Lee *et al.* reported micro patterned P(VDF:TrFE) based nano generators releasing 15μW power. Kymissis *et al*. used 16 sheets of PVDF connected in parallel in a sandwich structure in a shoe sole and was able to produce 1mJ/step. [10] Wang *et al.* used a synchronized switch harvesting on inductor (SSHI) rectifier for a PVDF stack configuration and harvested 11-13mW power. [11] Zirkl *et al* demonstrated an all printed matrix transducer array fabricated by screen printing an ink solution of piezoelectric copolymer P(VDF:TrFE). [12] Ink jet deposition of patterned metal layers on PVDF film to realize a scalable, bendable and low costing sensing system for large area artificial skin was reported by Seminara *et al*. [13]. Because of flexibility, piezoelectric polymers it can be integrated into devices for human body health monitoring, smart clothing such as shoes, and other motion harvesters applications. [14]

Rajala *et al*. measured the sensitivity of a PVDF transducer and observed a piezoelectric coefficient of 25.1 to 26.8 pC/N, using a shaker system. [15] In this work we report the use of a similar setup for determination of the piezoelectric sensitivity, and a motor-driven bending apparatus to measure harvesting of energy from bending deformation. In addition, a 3D bending model is used to analyze the results.

II. Experiment and Results

A: Piezo transducer design and electrical polarizatio

A transducer consists of four layers. Polyethylene terephthalate (PET, Melinex ST506 from DuPont) of 175 µm thickness was used as a substrate, printed conductive polymer PEDOT:PSS((poly(3,4ethylenedioxythiophene):poly(styrene sulfonic acid)) (Clevios SV 3 from Heraeus) act as bottom and top electrodes, and fluoropolymer P(VDF:TrFE), poly(vinylidenefluoride trifluoroethylene) (80:20) (see Ref. 12 for details) as a transducer material is sandwiched between the electrodes. Screen printing was used to deposit the transducer material and electrodes. The thickness of the transducer material was ~6µm for single layer and ~12 µm for double layer. The samples were annealed at 100 ºC for 10 minutes to evaporate solvents. Additionally, silver wiring was printed to electrically connect the transducer to the harvester circuitry, but is not part of the layer stack. Figure 1 shows the transducer schematic diagram.

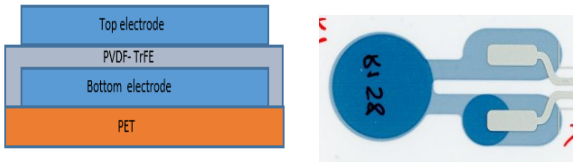

Figure 1: Structure of Piezo transducer

In contrast to PVDF films, the copolymer P(VDF:TrFE) crystallizes into the ferroelectric β-phase without the need of stretching or applying of very high electric fields. In P(VDF:TrFE), the crystallites have an electric dipole moment and are embedded in an amorphous matrix. After solution-processing of P(VDF: TrFE), however, the crystalline dipoles are randomly oriented and need to be aligned in order to have a nonzero overall polarization and thus show piezoelectricity. This alignment of crystalline dipoles is usually performed by applying an electric field via attached electrodes, forcing the crystalline dipoles to be reoriented towards the external field. This process is commonly referred to as poling. [7] The poling current I and voltage V are monitored and the polarization in the ferroelectric layer can be derived using the relation

$$P = \frac{1}{A} \cdot \int I \, dt, \qquad (1)$$

where, A is the area spanned by the electrodes. A triangular shaped alternating signal of frequency 1Hz was used for poling over several cycles until a saturation in the remanent polarization or charge, respectively, was observed (Figure 2). Plotting the polarization P over the voltage V gives the typical hysteresis loop of ferroelectrics (Figure 3). A PUND poling method was applied to separate the remanent polarization P_r due to crystalline dipole reorientation (dotted line) from the total displacement (solid line in Figure 3). To reach a high remanent polarization and thus piezoelectric coefficient (d_{33}), the poling voltage amplitude was chosen such as to apply about two times the coercive field strength E_r [16]

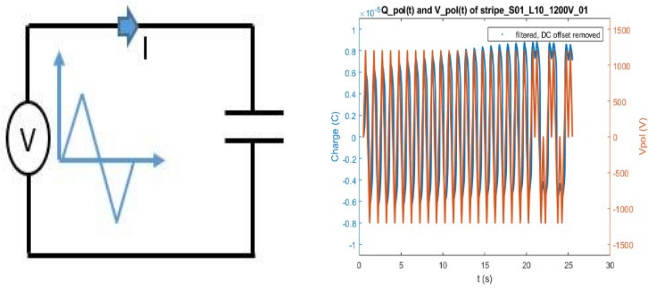

(a)

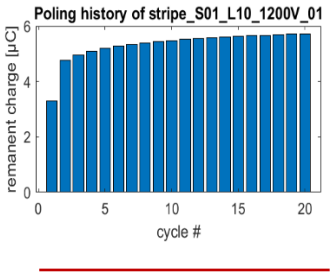

Figure 2: Poling of the ferroelectric P(VDF:TrFE). Poling charge as calculated from the monitored current and poling voltage (a); The remanent charge increases with every poling cycle and saturates, (b)

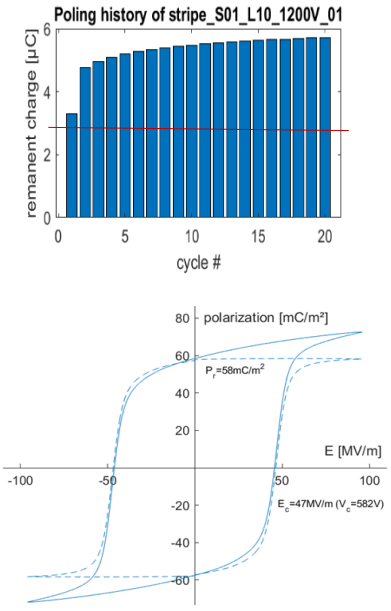

Figure 3: Typical hysteresis loop of the studied Piezoelectric transducer showing the remanent polarization P_r and coercive field strength E_r.

The coercive electric field strength measured was 47MV/m and the remanent polarization amounts to approximately 58mC/m^2. [12]

B: Sensitivity measurement bending and unbending setup

A type 4810 Brüel & Kjær mini-shaker was used for material characterization. The shaker has a piston of area of 1.56 $mm^2$and can generate a dynamic excitation force up to 10N and frequencies up to 18 KHz. A sinusoidal input for the shaker was provided with a Tektronix AFG3101 function generator. Two types of sensors were used during sensitivity measurements. The static force sensor, with sensitivity of 2.646 mV/N, was used to prevent the transducer from jumping off the stage during application of dynamic sinusoidal force. The dynamic force sensor, with sensitivity of 530.2mV/N, was used at varying amplitudes up to 10N for sensitivity measurements. The measurement set up using only the normal mode sensor was previously reported by Rajala *et al.* [15] Tuukkanen *et al.* [17] and Kärki *et al.* [18].

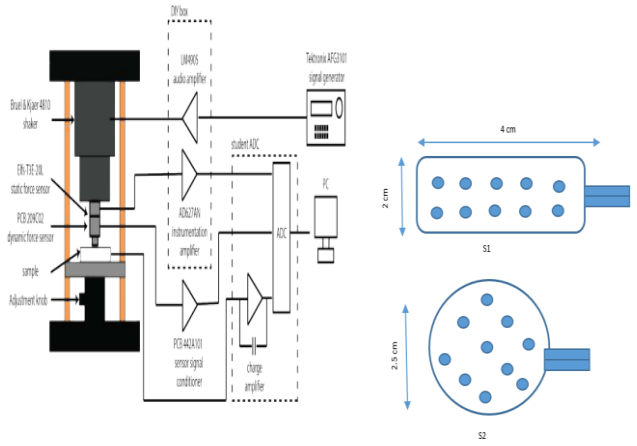

(a) (b)

Figure 4: A schematic drawing of measurement set up (a); piezo transducer with excitations point marked (S1 and S2) (b)

Two piezo transducers, designated here as S1 and S2, were selected for measurements and compared. (REF. Table 1). In the first set of measurements in normal mode, the transducer was placed in the metal plate. In the second set of measurements (bending mode), greater sample deformation was allowed, as shown in Figure 5. A sinusoidal signal of 1V peak to peak at 2 Hz frequency was applied as input to the shaker, which resulted in a force of approximately 1.4 N. The transducer was excited at 10 different positions. The same positions were excited from both sides of the transducer, resulting in total of 20 excitations per transducer in order to average out effects resulting from film roughness, increases the statistics and thus, decreases the effect of layer variations in the sensing layer thickness. The charge generated was measured by a charge amplifier. The sinusoidal were fit to the charge output curve and the dynamic force curve, and the sensitivity was obtained by dividing charge amplitude by force amplitude. [15]

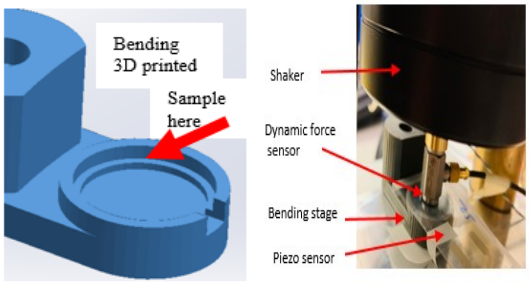

(a) (b)

Figure 5: Bending 3d setup (a); piezo transducer excited by mini-shaker (b)

Dynamic sensitivity is the charge generated based on the force applied in pC/N and was measured using both the normal and bending mode. The dynamic sensitivity is given by

$$Dynamic\ sensitivity = \frac{Q}{Dynamic\ force} \qquad (2) \quad [15]$$

TABLE 1: Dynamic sensitivity measurement results, reported as mean value ± standard deviation

Sample measured	**Dynamic sensitivity (pC/N)**	
	Normal mode	**Bend mode**
S1(8cm^2)	24.41±3.2	286±52
S2(7.85cm^2)	23.46±2.68	268±23.84

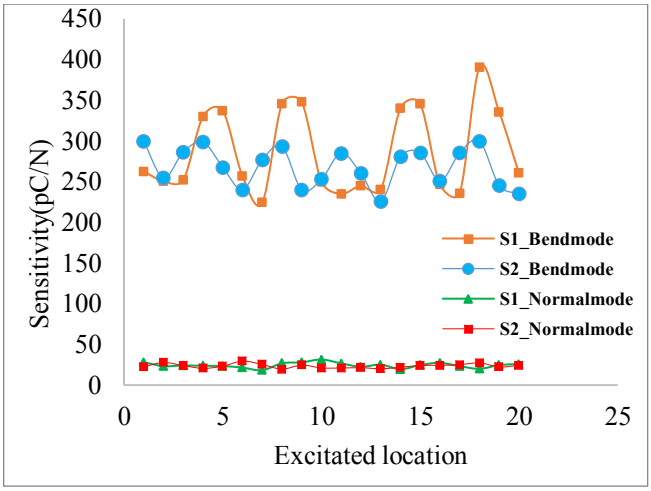

Figure 6: Sensitivity results with normal mode and bending mode

The charge generated by deformation of the material depends on the amount of force applied. Figure 7 shows generated charge as a function of applied force. Less force was required to generate a higher amount of charge using the bending stage, as it is primarily deformation that leads to charge generation. When using the bending stage 240pC charge was generated by applying 0.866 N force, compared to 27.5 pC charge from 1.4 N force using the rigid table. Rajala *et al.* [15] observed similar behavior.

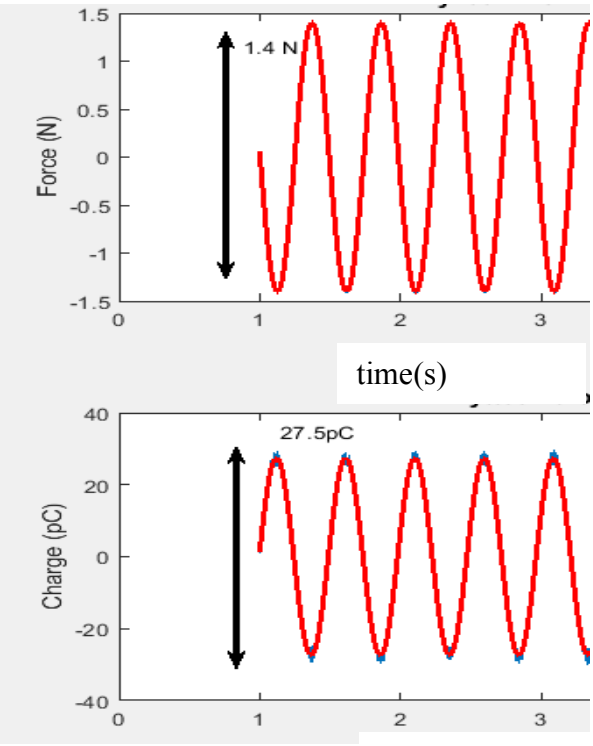

(a)

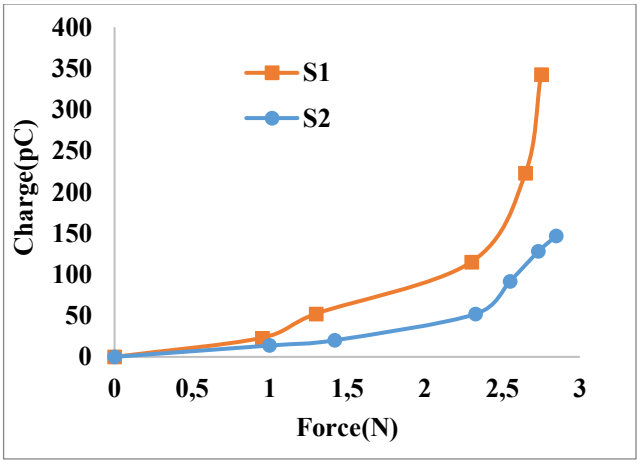

(b)

Figure 7: Charge generated based on force, normal mode (a);Graph plot of piezo transducer S1 and S2 (b)

C: Energy harvesting by angular bending

A measurement setup for energy harvesting by bending/ unbending is shown in figure 8. It consists of a servo motor that rotates from 0 to 180 ° and back with pulse width modulation, powered and controlled by an Arduino Uno microcontroller platform. A piezo transducer of 8cm^2 size was attached to the cylindrical shaft of the servo motor and this was flexed and unflexed as the motor rotated. The transducer output voltage response was 8 V peak to peak. (See figure 9(a)) The output response of the piezo transducer was measured with a 10 Mega ohm NI USB-4065 multimeter from National Instruments.

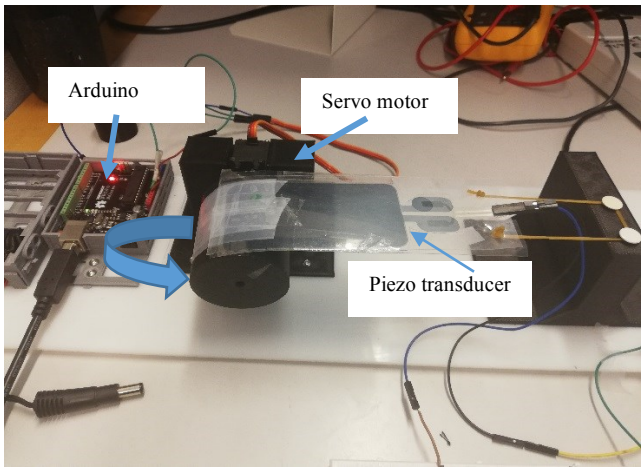

Figure 8: Setup for controlling Servomotor for angular bending

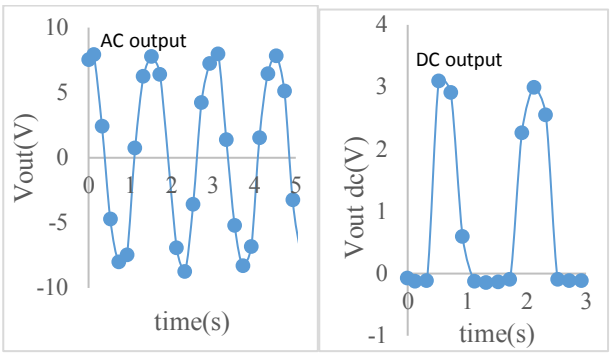

(a) (b)

Figure 9: Piezo transducer output Voltage Ac (a); DC (b)

A half wave rectifier circuit was integrated to the transducer to convert AC into DC. The DC obtained without smoothing capacitor is shown in Figure 9b. Figure 10 shows the charging characteristics of a smoothing/storage capacitor integrated to the system. The rectified voltage across a load of 10 M Ohm is 1.05V.

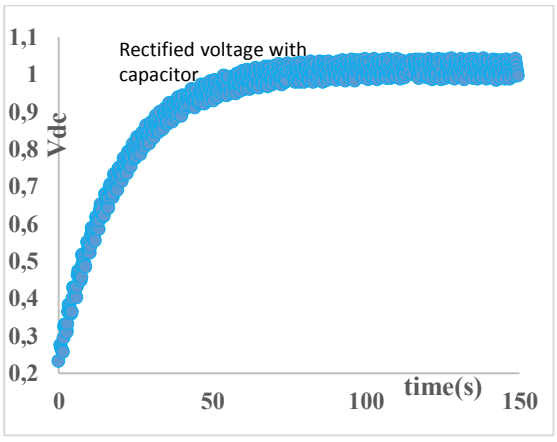

Figure 10: Rectified voltage with capacitor

The harvested energy is given by

$$E = \frac{1}{2}cv^2 \qquad (3)$$

where E is energy in Joule, C is capacitance in Farads and V is the voltage across the capacitor. This yields a harvested energy of 300 µJ.

D: Frequency dependency of piezo transducer

An energy harvester comprising a piezo transducer, rectifier circuit and storage capacitor was assembled; the block diagram is shown in Figure 11. Figure 12 shows photographs of a harvester circuit including a voltage doubler rectifier.

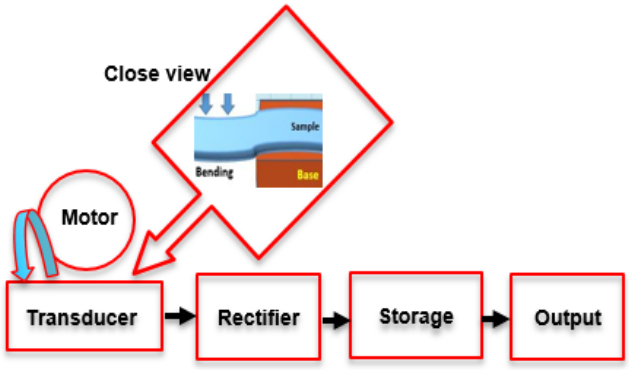

Figure 11: Variable frequency generator and energy harvesting system

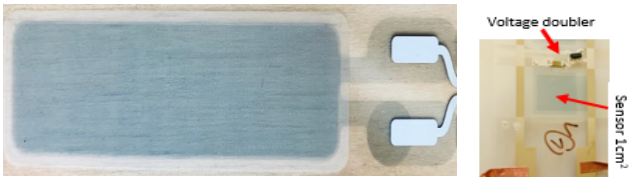

Figure 12: Piezo transducer A and B + Energy harvester

Two samples were investigated using the same excitation methods. The first transducer has an area of 14 cm^2 (7cm *2cm) while the second has area transducer has an area of 1cm^2 (1cm*1cm); both were connected to a voltage doubler rectifier. The motor was controlled by a VFD (variable frequency drive) in order to rotate at different speeds. One side of the piezo transducer was fixed while the other side can oscillate freely. A small mechanical load was attached to the shaft of the motor. As the motor rotates, the load hits the piezo transducer and bends it up and down, generating an AC voltage. Transducer 1 has AC output response of 6 V peak to peak (See figure 13) whereas transducer 2 generates 3 V peak to peak AC at 10 Hz frequency. A National Instruments 10 mega Ohm USB 4065 multimeter was used to measure the DC output.

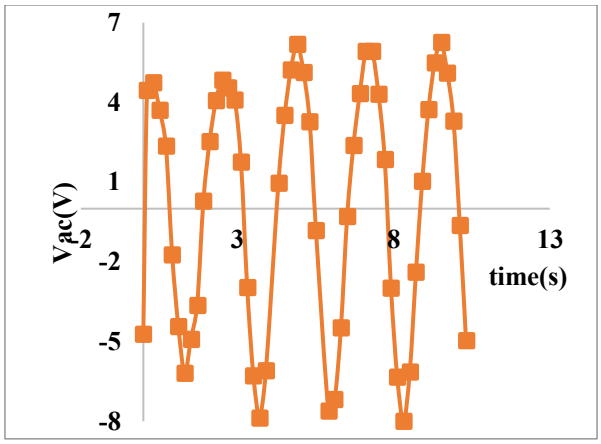

Figure 13: Response of Piezo Transducer A

As the output current of the transducer is low, it takes time to charge a capacitor greater than 100µF.This can be observed with a 470µF capacitor (angular bending test), which yielded an output voltage of 1.04 DC. Printed supercapacitors typically have an area specific capacitance of ca 100 mF/cm^2, with leakage current more or less proportional to capacitance. [19] Due to the small amount of energy from a single transducer in this work, the leakage current for a supercapcitor in the range of hundreds of mF would be comparable to the about of current generated. Therefore in these experiments we selected a commercial electrolytic capacitor of 22 µF and a printed 33 µF supercapacitor. This supercapacitor was fabricated using PET (polyethylene terephthalate) as substrate and graphite ink of about 40 µm thickness deposited by stencil printing, both as current collector and electrode. One Molar aqueous sodium chloride (NaCl) was used as an electrolyte and Dreamweaver cellulose paper as a separator.

The capacitor charging curves are shown below for transducers 1 and 2 for excitation 10 Hz to 50 Hz, showing that the rectified voltage and speed of charging are proportional to the excitation frequency. This implies that the fundamental frequency response of the transducers is more or less flat over this frequency range.

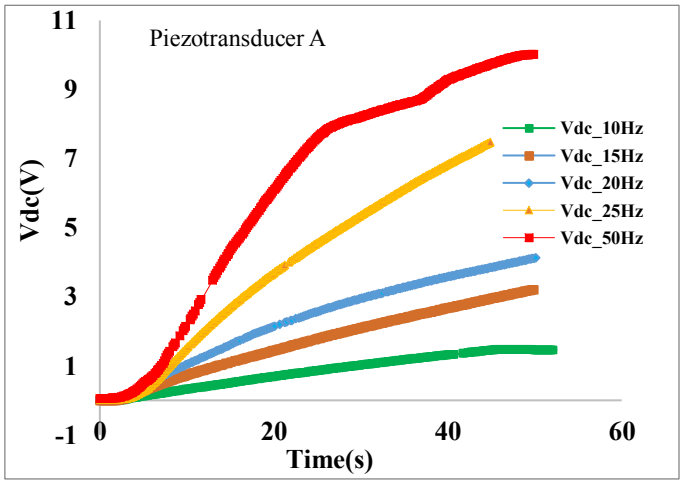

(a)

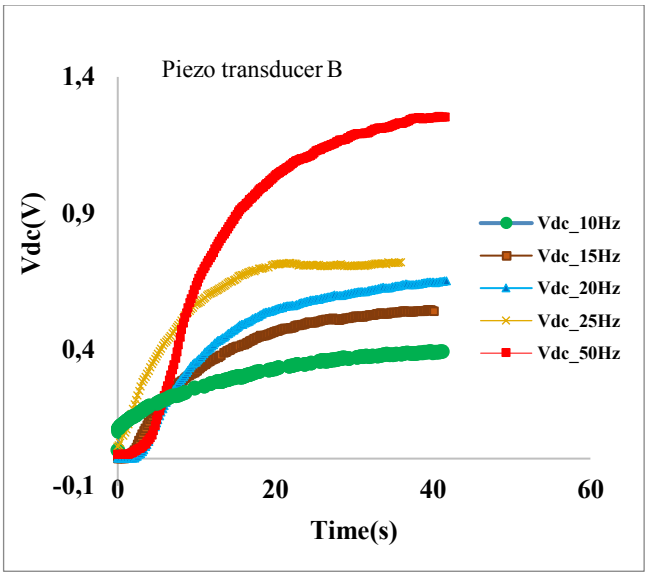

(b)

Figure 14: Rectified DC voltage of transducer A (a); transducer B (b) from 10 Hz to 50 Hz

The maximum voltage a single supercapacitor with aqueous electrolyte can withstand is about 1.2 V. In order to store the higher voltage generated by the transducer, 5 supercapacitors were connected in series, with total capacitance of 3µF as shown in Figure 15, and could be charged up to 7 V. Figure 15 also shows the charging curve for the series connected supercapacitor module at different frequencies.

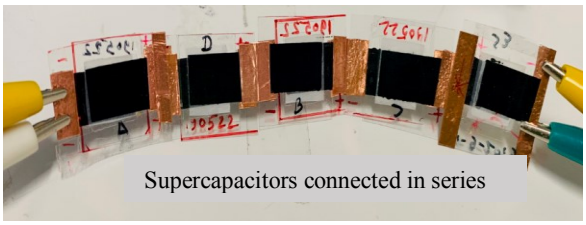

(a)

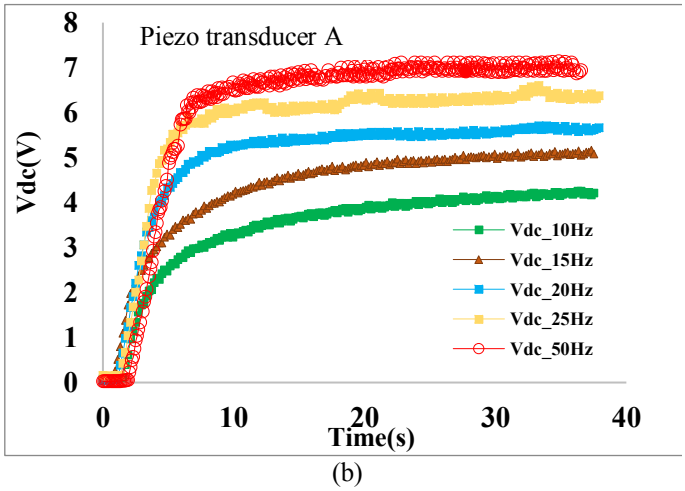

(b)

Figure 15: Five series connected supercapacitors (a); rectified voltages (b) from the harvester upon excitation in the test unit described in this work.

The rectified DC voltage increases in both transducers with the excitation frequency. The measurement was done with different piezo transducers and capacitor values. Transducer B has very low output compared to transducer 1, about 8 times less at 50 Hz due to its small area.

Table 2 summarizes the harvesting results. While it was not possible with a single transducer to charge a single 33 µF supercapacitor fully, due to the competition between charging and leakage current, both the electrolytic capacitor and the module were charged in less than a minute.

TABLE 2: Energy harvested from 10 Hz to 50 Hz

Frequency (Hz)	Piezo transducer A				Piezo transducer B	
	V_{dc} (V)		Energy (mJ)		V_{dc} (V)	Energy (mJ)
	Electrolytic capacitor(EC) 22µF	Super capacitor (SC) 3µF	EC	SC		33µF
10	1.45	4.2	0.02	0.0266	0.39	0.00251
15	3.19	5.07	0.11	0,0388	0.54	0.004811
20	4.08	5.7	0.18	0,049	0.65	0.006971
25	7.4	6.36	0.60	0,061	0.72	0.00855
50	10	7	1.12	0,073	1.25	0.0257

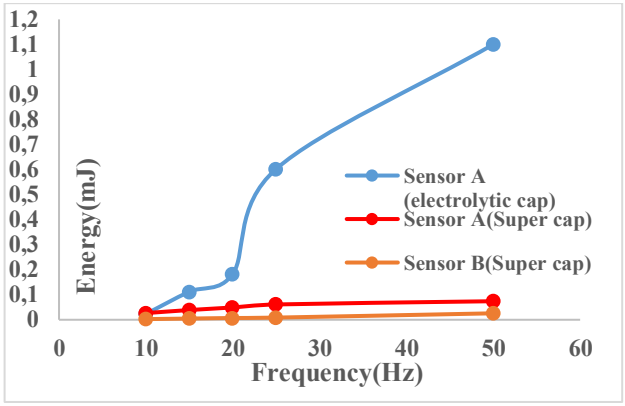

Figure 16: Energy harvested as a function of excitation frequency

This is sufficient energy to operate low power circuitry. We constructed a low power LED drive circuit using a CMOS 555 timer operated at 2V. The voltage stored in the capacitor was supplied to the LED driver circuit as shown in figure 17. The transistor acts as a switch and remains ON when the output pulse of the 555 timer drives the base of a transistor, and current flows to the LED. [20]

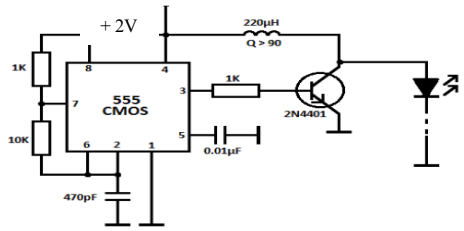

(a)

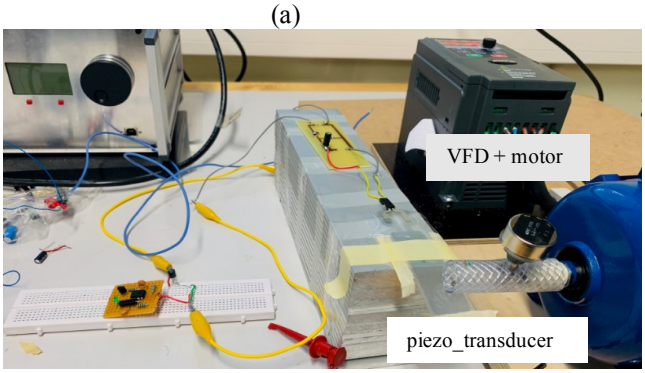

(b)

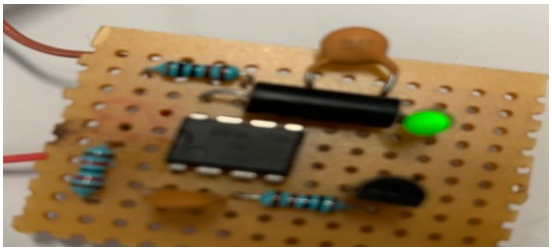

(c)

Figure 17: Schematic diagram of the LED driver circuit as published in [17] (a), photograph of the bending setup with LED driver circuit (b), and close-up of the LED driver circuit (c)

The operation voltage of the LED driver circuit was 1.85V and, current required to turn on LED was 6mA. Thus, the peak power generated by the circuit for short durations was measured i.e. P=1.85*6=11.1mW. It can be observed from Table 3 that the power generated can be used to operate a number of common low power portable devices.

TABLE 3: Power consumption of the portable devices [21] [3] [22] [23] [24]

Device		Power consumption (mW)
MP3 player		50-97
Wearable EEG		0.8
Cardiac pacemaker		0.05
Hearing aid		1
Respiratory rate meter		0,83
Heart rate meter		0,83
Blue tooth (sleep mode)		0.008
Wifi (sleep mode)		0.01
Carbon monoxide detector	Active	1.7
	Stand by	0,0018
Pagers		30

III. CONCLUSIONS

We have tested printed piezoelectric transducers based on P(VDF:TrFE) for their potential as energy harvesters in low power electronic devices. The piezoelectric sensitivity was a strong function of the freedom of the transducer to be deformed, with average sensitivity value (pC/N) in bending 11 to 12 times higher than when applying force when the sample was mounted on a rigid holder. The response varied from 20 - 31pC/N in a rigid architecture to 225.2-390 pC/N when bending was allowed. We have furthermore tested the energy harvesting potential of these transducers in a dedicated bending unit. In addition to determining the AC voltage generated by bending, an energy harvesting circuit on foil comprising transducer, voltage doubler rectifier and printed supercapacitor or electrolytic capacitor, respectively. The system was able to generate and store up to 1.12 mJ and deliver power of at least 11.1 mW, sufficient to drive an LED. This is sufficient power to drive a number of low power portable devices and confirms the potential of printed P(VDF:TrFE) as a potential means of harvesting energy from motion for distributed electronic devices.

References

[1] Y. Bai, J. Jantunen and J. Jari, "Energy harvesting research: The road from single source to multisource," *Advanced materials,* 2018.

[2] A. Harb, "Renewable Energy," *Energy harvesting : State -of-the-art,* vol. 36, 2011.

[3] J. Rocha, P. Silva and S. Mendez, "Energy Harvesting frompiezoelectric materials fully integrated in footwear," *IEEE,* vol. 57, 2010.

[4] M. Zirkl, G. Scheipl, B. Stadlober, C. Rendl, M. Haller and P. Hartmann, "Pyzoflex : a printed piezoelectric pressure sensing foil for human machine interfaces," *Proc. of SPIE,* vol. 8831, 2013.

[5] G. H. Heartling, "Ferroelectric Ceramics: History and Technology," *J. Am. Ceram. Soc,* vol. 82, no. 4, pp. 797-818, 1999.

[6] K. Rashmi, Jayarama, Navin Bappalige and R. Pinto, "A Review on vibration based piezoelectric energy harvesters," *Sahyadri International Journal of Research ,* vol. 3, no. 1, 2017.

[7] B. Stadlober, M. Zirkl and I. M. Vladu, "Route towards sustainable smart sensors: ferroelectric polyvinylidene fluoride-based materials and their integration in flexible electronics," *Royal society of Chemistry,* 2019.

[8] V. Bhavanasi, V. Kumar, K. Parida, J. Wang and S. P. Lee, "Enchanced piezoelectric energy harvesting performance of flexible PVDF-TrFE films with graphene oxide," *ACS Publications,* vol. 8, pp. 521-529, 2015.

[9] S. Dey, M. Purahmad, S. S. Ray and M. Dutta, "Investigation of PVDF-TrFE nanofibers for energy harvesting," *Nano Technology materials and Devices Conference,* 2013.

[10] J. Kymissis, C. Kendail, J. Paradiso and N. Gershenfeld, "Parasitic power harvesting in shoes," *IEEE,* 1998.

[11] Wang, "Piezoelectric energy harvesting utilizing human locomotion," *MSc Thesis, University of Miinnesota,* 2010.

[12] M. Zirkl, A. Sawatdee and U. Helbig, "An all printed ferroelectric active matrix sensor network based on only five functional materials forming a touchless control interface," *Advabced Materials,* vol. 23, pp. 2069-2074, 2011.

[13] L. Seminara, L. Pinna and M. Valle, "Piezoelectric polymer transducer arrays for flexible tactile sensors," *IEEE Sensors Journal,* vol. 1, no. 10, 2013.

[14] J. Zhao and Z. You, "A shoe embedded piezoelectric energy harvestor for wearable sensors," *Sensors,* vol. 14, no. 7, pp. 12497-12510, 2014.

[15] S. Rajala, S. Tuukkanen and J. Halttuen, "Characteristics of piezoelectric polymer film sensors with solution processable graphene based electrode materials," *IEEE Sensors Journal ,* vol. 15, 2015.

[16] J. Tressler, S. Alkoy and R. Newnham, "Piezoelectric sensors and sensor materials," *Journal of Electroceramics,* vol. 2, no. 4, pp. 257-272, 1998.

[17] S. Tuukkanen and S. Rajala, "Nanocellulose as a piezoelectric material," *IntechOpen,* 2018.

[18] S. Kärki, M. Kiiski, M. Mäntysalo and J. Lekkala, "A PVDF sensor with printed electrodes for normal and shear stress measurements on sole," *Fundamental and Applied Metrology,* 2009.

[19] S. Lehtimäki , M. Li, J. Salomaa, J. Pörhönen, A. Kalanti, S. Tuukkanen, P. Heljo, K. Halonen and D. Lupo, "Performance of printable supercapacitors in an RF energy harvesting circuit," *Electrical Power and Energy Systems,* vol. 58, pp. 42-46, 2014.

[20] "Available online" https://www.electroschematics.com/6754/led-driver-with-555-timer/"".

[21] V. Lenov, Energy harvesting for self powered wearable devices, Springer US, 2011, pp. 27-49.

[22] R. Vullers, R. V. Schaijk, I. Doms, C. V. Hoof and R. Mertens, "Micropower energy harvesting," *Solid-State Electronics,* vol. 12, no. 11, 2008.

[23] Snehalika and U. Bhasker, "Piezoelectric energy harvesting from shoels of soldier," *IEEE Power electronics, Intelligent control and Energy Systems,* pp. 1-5, 2016.

[24] V. Bhatnagar and P. Owende, "Energy harvesting for assistive and mobile applications," *Energy Science and Engineering,* vol. 3, pp. 153-173, 2015.

[25] J. Lekkala, J. Tuppurainen and M. Paajanen, "Material and operational properties of large area membrane type sensors for smart environments," *XVII IMEKO World Congress,* 2003.

[26] A. V. Shirinov and W. K. Schomburg, "Pressure sensor from a PVDF film," *Sensors and Actuators,* vol. 142, pp. 48-55, 2008.

[27] S. Lehtimäki, M. Li, J. Salomaa, P. Juho, A. Kalanti, S. Tuukkanen, P. Heljo, K. Halonen and D. Lupo, "Performance of printable supercapacitors in an RF energy harvesting circuit," *Electrical Power and Energy Systems,* vol. 58, pp. 42-46, 2014.